

A SUBSHIFT OF FINITE TYPE
IN THE TAKENS-BOGDANOV BIFURCATION
WITH D_3 SYMMETRY

KARSTEN MATTHIES

Received: November 5, 1998

Revised: August 30, 1999

Communicated by Bernold Fiedler

ABSTRACT. We study the versal unfolding of a vector field of codimension two, that has an algebraically double eigenvalue 0 in the linearisation of the origin and is equivariant under a representation of the symmetry group D_3 . A subshift of finite type is encountered near a clover of homoclinic orbits. The subshift encodes the itinerary along the three different homoclinic orbits. In this subshift all those symbol sequences are realized for which consecutive symbols are different. In the parameter space we also locate a transcritical, three different Hopf and two global (homoclinic) bifurcations.

1991 Mathematics Subject Classification: 34C28, 58F14

Keywords and Phrases: Takens-Bogdanov, subshift of finite type, symmetry, homoclinic orbit

1 INTRODUCTION

A vector field has a Takens-Bogdanov point, if there is a Jordan block $\begin{pmatrix} 0 & 1 \\ 0 & 0 \end{pmatrix}$ in the linearisation of a steady state and if certain nondegeneracy conditions are fulfilled. This codimension two degeneracy with its unfolding is a key to understand several phenomena in dynamical systems (see [17, 3] and textbooks like [13]). Takens-Bogdanov points can also serve as a starting point for the path following in two-parameter flows of global Hopf bifurcation [6] and homoclinic orbits [7]. One parameter families of homoclinic orbits are

created at Takens-Bogdanov points of two-parameter flows. Hence these bifurcation points play the same role for the creation of homoclinic orbits in two-parameter flows as Hopf bifurcation for periodic solutions in one-parameter flows. Near homoclinic orbits several bifurcations to other bounded solutions may occur. Thus Takens-Bogdanov points are important organizing centers for the bifurcation analysis of dynamical systems. Suppose the dynamical system $\dot{x} = f(x)$ has constraints given by an equivariance under a symmetry group Γ , i.e. $f(\gamma x) = \gamma f(x)$, for $\gamma \in \Gamma$. Then one often finds complicated bifurcation diagrams even at simple bifurcations, [11].

Similarly at the Takens-Bogdanov point with D_3 symmetry the dynamics are much richer than in the non-symmetric case. Applications are given to systems of three coupled oscillators in a ring. The results could be also applied to mode interactions for pattern formation in convection problems, where solutions with D_3 symmetry exist [12]. We will encounter a subshift of finite type, which is a novel dynamical feature in a bifurcation problem of dynamical systems defined by a vector field. Whereas in many bifurcations one can encounter Smale horseshoes giving rise to a full shift, the existence of a subshift of finite type is a rare phenomenon.

A subshift $\sigma(x_n)_{n \in \mathbf{Z}} = (x_{n+1})_{n \in \mathbf{Z}}$ of finite type on three symbols $\{1, 2, 3\}$ is defined on

$$X_A = \{(x_n)_{n \in \mathbf{Z}} \mid x_n \in \{1, 2, 3\}, a_{x_n, x_{n+1}} = 1\}$$

where $A = (a_{i,j})_{i,j \in \{1,2,3\}}$ is a 3×3 matrix with entries 0 and 1. The topology of X_A is defined as the product topology of the discrete set of symbols $\{1, 2, 3\}$. A subshift of finite type allows only those symbol sequences, for which consecutive symbols x_n, x_{n+1} are compatible with the transition matrix A . The symmetry group D_3 will act on X_A in the following manner

$$\begin{aligned} \text{'flip':} \quad \kappa((x_n)_{n \in \mathbf{Z}}) &= (\tilde{\kappa} x_n)_{n \in \mathbf{Z}} \text{ with } \tilde{\kappa} 1 = 1, \tilde{\kappa} 2 = 3, \tilde{\kappa} 3 = 2 \\ \text{'rotation':} \quad \gamma((x_n)_{n \in \mathbf{Z}}) &= (x_{n+1 \bmod 3})_{n \in \mathbf{Z}}. \end{aligned} \quad (1)$$

The bifurcation analysis will be reduced in section 2 to the discussion of a vector field on $\mathbf{R}^4 \cong \mathbf{C}^2$, where D_3 acts as

$$\begin{aligned} \text{'flip':} \quad \kappa(v, w) &= (\bar{v}, \bar{w}) \\ \text{'rotation':} \quad \gamma(v, w) &= (\exp(i \frac{2\pi}{3})v, \exp(i \frac{2\pi}{3})w). \end{aligned} \quad (2)$$

A vector field in normal form can be derived. Using additional parameters (μ_1, μ_2) to unfold the singularity the normal form is generically given - up to time reversal - by

$$\begin{aligned} \dot{v} &= w \\ \dot{w} &= \mu_1 v + \mu_2 w + \bar{v}^2 - \bar{v}\bar{w} + [A|v|^2 + B|w|^2 + C(v\bar{w} + \bar{v}w)]v + D|v|^2 w. \end{aligned} \quad (3)$$

A bifurcation diagram describing the complete plane of unfolding parameters is given in figure 1. The main result of this paper is formulated in theorem 1. It states the existence of a special form of a horseshoe for an open set of parameter

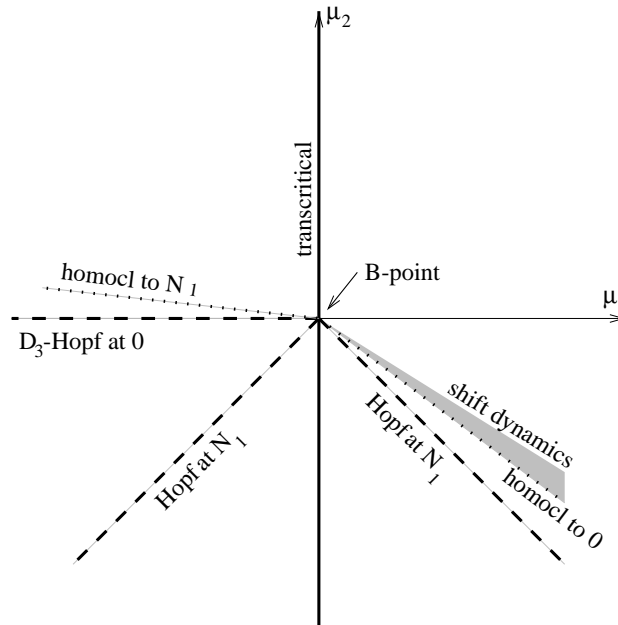


Figure 1: Bifurcation diagram in parameter space: transcritical bifurcation of steady states (bold line), three kind of Hopf bifurcation (dashed lines), two different homoclinic bifurcations (dotted lines) and shift dynamics (shaded area).

values. Later we will rigorously define three Poincaré sections $S_1^{in}, S_2^{in}, S_3^{in}$ as sections along three coexisting homoclinic orbits biasymptotic to the origin. P will be the return map on $S_1^{in} \cup S_2^{in} \cup S_3^{in}$.

THEOREM 1 *For $0 < \mu_2 + \frac{6}{7}\mu_1$ small, $\mu_1 > 0$, there exists an invariant hyperbolic Cantor set $C \subset S_1^{in} \cup S_2^{in} \cup S_3^{in}$ such that the return map $P : C \rightarrow C$ induced by the flow of (3) is topological conjugate to the irreducible subshift of*

finite type with transition matrix $A = \begin{pmatrix} 0 & 1 & 1 \\ 1 & 0 & 1 \\ 1 & 1 & 0 \end{pmatrix}$. Here means topological

conjugacy that there exists an homeomorphism $\tau : C \rightarrow X_A$ such that $\tau P = \sigma \tau$ on C .

Furthermore P and τ can be chosen to be D_3 -equivariant, when using the representation (2) on C and (1) on X_A . C is D_3 -invariant.

So in fact we have a D_3 -subshift of finite type as defined in [8]. Neither the incomplete bifurcation diagram in figure 1 nor theorem 1 depend on the coefficients A, B, C, D and other higher order terms. In the bifurcation diagram the lines will be bended to curves by a near-identity diffeomorphism. This is peculiar to the case of D_3 symmetry. When the system has some other symmetry

group like $O(2)$ [4] or D_4 [1] many more parameters and several different bifurcation diagrams have to be discussed. Thus our analysis can only be a first step to a general analysis of D_n equivariant Takens-Bogdanov singularities, where one might hope to encounter the $O(2)$ case as a limit.

The rest of the paper is organized as follows. In section 2 we give the Taylor expansion near the origin of a generic vector field equivariant under (2) at the Takens-Bogdanov point, derive a normal form up to third order and unfold it. We discuss the basic dynamical behavior in section 3, i.e. we analyze steady states, Hopf bifurcations and the dynamics in invariant subspaces including homoclinic orbits. The existence of the subshift will be proved in section 4, where we use a definition of a general horseshoe. In the last section 5 we will discuss some further numerical studies and applications.

2 D_3 -EQUIVARIANT VECTOR FIELDS AND NORMAL FORMS

Before giving a Taylor expansion near the singularity we first use some representation theory to justify the representation like in (2). There are in general two possibilities that a representation space of a compact Lie group Γ admits a non-diagonalizable Γ -equivariant linearisation A at the origin. Similar to chapter XVI of [11] there must be a Γ -invariant subspace W , that is either of the form $V \oplus V$, where V is absolutely irreducible, or that is irreducible but not absolutely irreducible. The second case is not possible for the Takens-Bogdanov singularity. The linearisation A contains the nilpotent matrix $\begin{pmatrix} 0 & 1 \\ 0 & 0 \end{pmatrix}$. Suppose W is irreducible but not absolutely irreducible, then $A(W) = 0$ or $A(W)$ is isomorphic to W [11, Lemma XII.3.4]. But if $A|_W$ contains the nilpotent Jordan block then $A : W \rightarrow A(W)$ cannot be an isomorphism. Hence $A|_W = 0$ and this is in contradiction that the Jordan block is non-zero. So we use a representation of the form $V \oplus V$. When choosing for V the standard representation of D_3 on $\mathbf{C} \cong \mathbf{R}^2$ we get the representation (2).

PROPOSITION 2 (i) *The ring of all D_3 -invariant germs acting on $\mathbf{C} \oplus \mathbf{C}$ as in (2) is generated by*

$$s_1 = v\bar{v}, \quad s_2 = w\bar{w}, \quad s_3 = v\bar{w} + \bar{v}w \quad \text{and}$$

$$t_j = v^j w^{3-j} + \bar{v}^j \bar{w}^{3-j}, \quad j \in \{0, \dots, 3\}$$

(ii) *The module of D_3 -equivariant smooth mappings of $\mathbf{C} \oplus \mathbf{C} \rightarrow \mathbf{C} \oplus \mathbf{C}$ is generated by*

$$g_0 = \begin{pmatrix} v \\ 0 \end{pmatrix}, \quad g_1 = \begin{pmatrix} 0 \\ v \end{pmatrix}, \quad g_2 = \begin{pmatrix} w \\ 0 \end{pmatrix}, \quad g_3 = \begin{pmatrix} 0 \\ w \end{pmatrix} \quad \text{and}$$

$$f_j = \begin{pmatrix} \bar{v}^j \bar{w}^{2-j} \\ 0 \end{pmatrix}, \quad h_j = \begin{pmatrix} 0 \\ \bar{v}^j \bar{w}^{2-j} \end{pmatrix}, \quad j \in \{0, 1, 2\},$$

i.e. all D_3 -equivariant smooth germs of mappings $h : \mathbf{R}^4 \rightarrow \mathbf{R}^4$ can be written in the form $h(v, \bar{v}, w, \bar{w}) = p_0g_0 + p_1g_1 + p_2g_2 + p_3g_3 + q_0f_0 + q_1f_1 + q_2f_2 + r_0h_0 + r_1h_1 + r_2h_2$ where $p_0, \dots, p_3, q_0, q_1, q_2, r_0, r_1, r_2$ are smooth function germs of $s_1, s_2, s_3, t_0, \dots, t_3$.

Proof: For polynomials the completeness of the generators can be checked by lengthy by-hand calculations or by computer algebra, see [9]. These are then by Poénaru’s theorem also the generators of the module of germs of mappings. \square Then a general D_3 -Takens-Bogdanov point has the following Taylor expansion up to third order with real coefficients a_1, b_1, \dots :

$$\begin{aligned} \dot{v} &= w + a_1\bar{v}^2 + b_1\bar{v}\bar{w} + c_1\bar{w}^2 \\ &\quad + v(d_1v\bar{v} + e_1w\bar{w} + f_1(v\bar{w} + \bar{v}w)) \\ &\quad + w(g_1v\bar{v} + h_1w\bar{w} + i_1(v\bar{w} + \bar{v}w)) \\ \dot{w} &= a_2\bar{v}^2 + b_2\bar{v}\bar{w} + c_2\bar{w}^2 \\ &\quad + v(d_2v\bar{v} + e_2w\bar{w} + f_2(v\bar{w} + \bar{v}w)) \\ &\quad + w(g_2v\bar{v} + h_2w\bar{w} + i_2(v\bar{w} + \bar{v}w)). \end{aligned} \tag{4}$$

First we try to remove as many second order terms as possible, therefore we choose a general near-identity D_3 -equivariant coordinate change.

$$\begin{aligned} v &= v' + \alpha_1\bar{v}^2 + \beta_1\bar{v}\bar{w} + \gamma_1\bar{w}^2 \\ w &= w' + \alpha_2\bar{v}^2 + \beta_2\bar{v}\bar{w} + \gamma_2\bar{w}^2 \end{aligned}$$

We rewrite (4) in the new coordinates and this yields to

$$\begin{aligned} \dot{v}' &= w' + (a_1 + \alpha_2)\bar{v}'^2 + (b_1 + \beta_2 - 2\alpha_1)\bar{v}'\bar{w}' + (c_1 + \gamma_2 - \beta_1)\bar{w}'^2 \\ &\quad + v'(\tilde{d}_1v'\bar{v}' + \tilde{e}_1w'\bar{w}' + \tilde{f}_1(v'\bar{w}' + \bar{v}'w')) \\ &\quad + w'(\tilde{g}_1v'\bar{v}' + \tilde{h}_1w'\bar{w}' + \tilde{i}_1(v'\bar{w}' + \bar{v}'w')) \\ \dot{w}' &= a_2\bar{v}'^2 + (b_2 - 2\alpha_2)\bar{v}'\bar{w}' + (c_2 - \beta_2)\bar{w}'^2 \\ &\quad + v'(\tilde{d}_2v'\bar{v}' + \tilde{e}_2w'\bar{w}' + \tilde{f}_2(v'\bar{w}' + \bar{v}'w')) \\ &\quad + w'(\tilde{g}_2v'\bar{v}' + \tilde{h}_2w'\bar{w}' + \tilde{i}_2(v'\bar{w}' + \bar{v}'w')) \end{aligned} \tag{5}$$

where the $\tilde{}$ terms depend on the original term, a_i, b_i, c_i and $\alpha_i, \beta_i, \gamma_i$ for $i = 1, 2$. By choosing

$$\alpha_1 = \frac{1}{2}(b_1 + c_2), \alpha_2 = -a_1, \beta_1 = 0, \beta_2 = c_2, \gamma_1 = 0, \gamma_2 = -c_1$$

we can remove all second order terms in the first component and \bar{w}'^2 in the second component in (5). All the third order terms are $O(2)$ -equivariant. Thus we can use exactly the same coordinate change as Dangelmayr and Knobloch [4] (after removing the second order terms) without affecting the lower order terms to get the following simplified system:

$$\begin{aligned} \dot{v} &= w \\ \dot{w} &= E\bar{v}^2 + F\bar{v}\bar{w} + [A|v|^2 + B|w|^2 + C(v\bar{w} + \bar{v}w)]v + D|v|^2w, \end{aligned}$$

where $E = a_2, F = b_2 + 2a_1, A = \tilde{d}_2, B = \tilde{d}_2 - \tilde{g}_1 + \tilde{f}_1 - 2\tilde{i}_2, C = \tilde{d}_1 + \tilde{f}_2$ and $D = \tilde{d}_1 + \tilde{g}_2$. We use an unfolding to describe the behavior of generic families of vector fields near the singular point. Even if there is not a general method to unfold the whole vector field, the linear part can be unfolded by $\begin{pmatrix} 0 & 0 \\ \mu_1 & \mu_2 \end{pmatrix}$ such that all nearby linear parts can be reached up to conjugation [2]. After scaling v, w, t and possibly a time-reversal we can set generically $E = 1, F = -1$, if the transformed second order terms are nonzero. Then we get the normal form as in equation (3):

$$\begin{aligned} \dot{v} &= w \\ \dot{w} &= \mu_1 v + \mu_2 w + \bar{v}^2 - \bar{v}\bar{w} + [A|v|^2 + B|w|^2 + C(v\bar{w} + \bar{v}w)]v + D|v|^2 w. \end{aligned}$$

3 BIFURCATIONS

Standard computations show some symmetry breaking bifurcations. Here especially the behavior inside the flow-invariant fixed point space $\text{Fix}(\kappa) = \{(v, w) | \kappa(v, w) = (v, w)\} = \{(v, w) | v, w \in \mathbf{R}\}$ will be considered. The same dynamics can be encountered in the rotated spaces $\gamma\text{Fix}(\kappa)$ and $\gamma^2\text{Fix}(\kappa)$. The bifurcation inside these planes is a Takens-Bogdanov bifurcation, in which the origin remains a singular point. This was analyzed by Hirschberg and Knobloch [14].

In general cubic and quintic terms cannot be neglected in Hopf bifurcation with D_3 symmetry. But in our situation the higher order terms are not important as long μ_1, μ_2 are small enough. To see this we have to perform the normal form calculations including these terms. The terms involving e.g. A, B, C, D are all of higher order in μ_1, μ_2 and hence can be neglected in a small neighborhood of 0 in the μ_1, μ_2 plane. For illustration we consider a Hopf bifurcation of the origin at $\mu_2 = 0, \mu_1 < 0$ inside $\text{Fix}(\kappa)$. After calculating a normal form for Hopf bifurcation like in [13] the direction of branching is determined by the sign of the term $a = -\frac{1}{8|\mu_1|} + \frac{2C+D}{8}$. So the higher order terms can be neglected inside a neighborhood of $(0, 0)$ in parameter space (μ_1, μ_2) . Similar results hold for the other bifurcations too. We suppress therefore the dependence on these terms. They only bend some lines in the bifurcation diagram to curves by a near-identity diffeomorphism. See also figure 1.

- The only stable feature is the origin for $\mu_1, \mu_2 < 0$.
- For $\mu_1 = 0$ there is a transcritical bifurcation of secondary steady state $N_1 = (-\mu_1, 0)$ and the rotated points $N_2 = \gamma N_1, N_3 = \gamma^2 N_1$ each with isotropy \mathbf{Z}_2 .
- For $\mu_2 = 0, \mu_1 < 0$ the spectrum of the origin is purely imaginary and the system undergoes a D_3 -Hopf bifurcation [11], where three different types of periodic solutions appear (isotropy type $\tilde{\mathbf{Z}}_3$ for $\mu_2 < 0$; solutions of

isotropy type $\tilde{\mathbf{Z}}_2$ and inside $\text{Fix}(\kappa)$ of isotropy type \mathbf{Z}_2 both for $\mu_2 > 0$; all these solutions are of saddle type).

- For $\mu_2 = \mu_1 < 0$ N_1, N_2, N_3 undergo Hopf bifurcations, where the imaginary eigenvalues have eigenvectors outside the invariant subspaces and the solutions have isotropy $\tilde{\mathbf{Z}}_2$.
- For $0 > \mu_2 = -\mu_1$ N_1, N_2, N_3 undergo Hopf bifurcations inside the invariant subspaces, i.e. the periodic orbit have isotropy \mathbf{Z}_2 .
- For some curve with $\mu_2 \approx -\frac{6}{7}\mu_1, \mu_1 > 0$ there exists an orbit inside $\text{Fix}(\kappa)$ homoclinic to 0, see [14].
- Similar there are orbits homoclinic to N_1, N_2, N_3 for $\mu_2 \approx -\frac{1}{7}\mu_1, \mu_1 < 0$.

For the homoclinic orbits we have even nearly explicit expressions. Scaling the equation (3)

$$\tau = \epsilon t, v = \epsilon^2 x, w = \epsilon^3 y, \mu_1 = \epsilon^2 \nu_1, \mu_2 = \epsilon^2 \nu_2.$$

and $\dot{} = \frac{d}{d\tau}$ give

$$\begin{aligned} \dot{x} &= y \\ \dot{y} &= \nu_1 x + \bar{x}^2 + \epsilon(\nu_2 y - \bar{x}\bar{y}) + O(\epsilon^2). \end{aligned} \tag{6}$$

Letting $\epsilon = 0$ the system has an explicit homoclinic orbit for $\nu_1 > 0$ inside $\text{Fix}(\kappa)$:

$$q_0(t) = \begin{pmatrix} x_q(t) \\ y_q(t) \end{pmatrix} = \begin{pmatrix} -\frac{3\nu_1}{2} \left(1 - \tanh^2\left(\frac{\sqrt{\nu_1}}{2}t\right)\right) \\ \frac{3\nu_1}{2}\sqrt{\nu_1}\text{sech}^2\left(\frac{\sqrt{\nu_1}}{2}t\right)\tanh\left(\frac{\sqrt{\nu_1}}{2}t\right) \end{pmatrix}.$$

Using the Melnikov method, see e.g. Guckenheimer and Holmes [13], we can then compute parameter values for which the homoclinic orbit persists for $\epsilon > 0$ to get the above results.

By symmetry there are homoclinic orbits biasymptotic to the origin inside the other two invariant fixed point spaces $\gamma\text{Fix}(\kappa)$ and $\gamma^2\text{Fix}(\kappa)$ for the same parameter values too. So there exists a ‘clover’ like structure of homoclinic orbits, see figure 2.

4 GENERAL HORSESHOES AND PROOF OF THEOREM 1

In this section we prove the existence of the subshift of finite type near the clover of homoclinic orbits. We will compute a Poincaré map near the homoclinic orbits with varying unfolding parameters μ_1 and μ_2 . For each of the three homoclinic orbits we define an ‘in’ and an ‘out’ section, called S_i^{in} and S_i^{out} (figure 3). The return map $P : S_1^{in} \cup S_2^{in} \cup S_3^{in} \rightarrow S_1^{in} \cup S_2^{in} \cup S_3^{in}$ is discussed by dividing it into local parts near the steady state, which can be described by

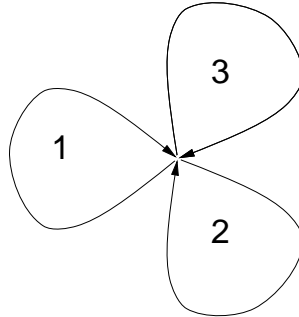


Figure 2: A sketch of the clover of homoclinic orbits. The three orbits lie all in different planes, which intersect only in the origin.

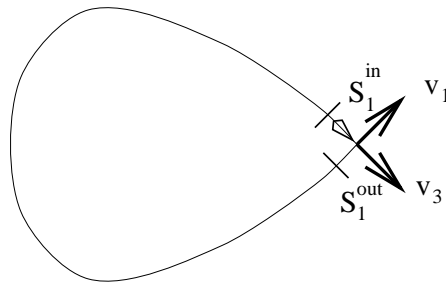


Figure 3: The sections S_1^{out} and S_1^{in} at the homoclinic orbit projected to $\text{Fix}(\kappa)$.

its linearisation (lemma 4) and global parts along the homoclinic orbit. This technique can also be used to analyze several other homoclinic bifurcations, see for example the textbook [10].

Before we give the technical details of the analysis of P , we describe the geometric idea: The sections S_i^{in} and S_i^{out} are cubes in \mathbf{R}^3 . We identify those regions in S_i^{out} , which have a preimage in some S_i^{in} under the local maps (see figure 4). Similarly we compute the regions in S_i^{in} , which are mapped by the local maps to some S_i^{out} (see figure 5). The global map P will map the cube in figure 4 to the cube in figure 5.

For appropriately chosen parameters (μ_1, μ_2) the slabs marked '2' and '3' in figure 4 will intersect the slabs '2' and '3' in figure 5. We can then show that there is a Smale horseshoe in three dimensions in the upper half of the cube. But because of the symmetry we have three copies of these cubes and the possible itineraries inside the invariant set are more complicated. In the figures 4 and 5 the sections of the homoclinic orbit marked '1' in figure 2 are shown. The trajectories of points in the regions '2' and '3' in figure 4 were in the sections S_2^{in} and S_3^{in} before. In the same way the slabs '2' and '3' in figure 5 are those regions, where the forward orbit will reach the section S_2^{out} and

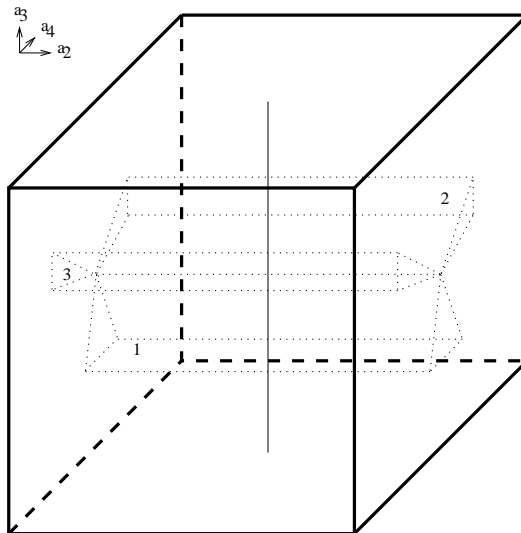


Figure 4: The section S_1^{out} with the images of S_1^{in} , S_2^{in} and S_3^{in} . The line in the middle is the section with $\text{Fix}(\kappa)$.

S_3^{out} next. Hence the itineraries, described in the figures 4 and 5, have first a symbol ‘2’ or ‘3’ then the symbol ‘1’, because they are now at the homoclinic orbit with symbol ‘1’, and then proceed with ‘2’ or ‘3’. At the other sections there is the same behavior after following once along the homoclinic loop: The trajectories of points inside the invariant set will lead to another section and hence to another symbol. Therefore the subshift described in theorem 1 can be realized, but no other infinite symbol sequences.

To rigorously prove the existence of the subshift, we describe briefly the notion of a general horseshoe in \mathbf{R}^3 following Katok and Hasselblatt [15]. First we explain the meaning of ‘full intersection’. Then using cone conditions we give precise meaning to ‘horizontal expansion’ and ‘vertical contraction’. We prove a technical lemma to justify the complete linearisation near the steady state before computing the local and global maps.

We will consider a *rectangle* $\Delta = D_1 \times D_2 \subset \mathbf{R} \oplus \mathbf{R}^2 = \mathbf{R}^3$ where D_1 and D_2 are discs. The projections on the components are denoted by π_1 (“horizontal”) and π_2 (“vertical”). Let $\Delta \subset U \subset \mathbf{R}^3$ be a rectangle and $f : U \rightarrow \mathbf{R}^3$ be a diffeomorphism. Then we call a connected component $S' = fS \subset \Delta \cap f\Delta$ *full*, if

1. $\pi_2(S) = D_2$,
2. for all $z \in S, \pi_1|_{f(S \cap (D_1 \times \pi_2(z)))}$ is a bijection onto D_1 .

The first condition implies that S reaches completely along the vertical direction and second one that the image of every horizontal fiber in S meets Δ and

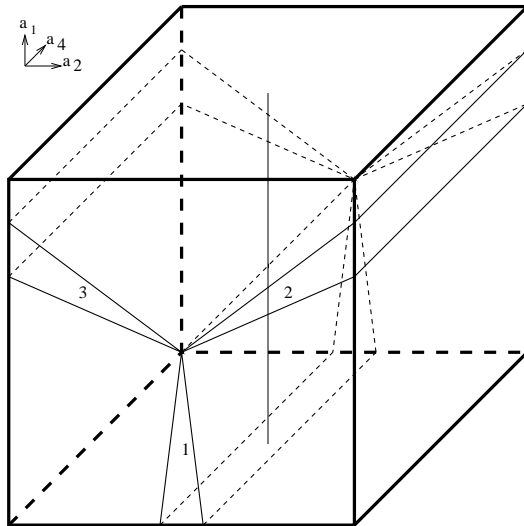


Figure 5: The section S_1^{in} where the preimages of S_1^{out} , S_2^{out} and S_3^{out} are the dotted slabs.

traverses it completely.

Next we introduce cone conditions. A horizontal s -cone H_x^s is defined by $H_x^s = \{(u, v) \in T_x \mathbf{R}^3 \mid \|v\| \leq s\|u\|\}$, similarly a vertical s -cone V_x^s by $V_x^s = \{(u, v) \in T_x \mathbf{R}^3 \mid \|u\| \leq s\|v\|\}$ at $x \in \mathbf{R}^3$ for some s . A map f preserves a family H_x of horizontal cones for $x \in U \subset \mathbf{R}^3$, if $Df_x(H_x) \subset \text{int}(H_{f(x)}) \cup \{0\}$. It is called expanding on a horizontal cone family H_x , if $\|Df_x \xi\| \geq \mu \|\xi\|$ for $\xi \in H_x$ and some fixed $\mu > 1$. We want to express a contraction property in the vertical direction, thus we consider f^{-1} on vertical cone families. It preserves the vertical cone family V_x , if $Df_x^{-1}(V_{f(x)}) \subset \text{int}(V_x) \cup \{0\}$ and f^{-1} expands them, if $\|Df_x^{-1} \xi\| \geq \lambda^{-1} \|\xi\|$ for $\xi \in V_{f(x)}$ and some uniform $\lambda < 1$. Then the appropriate generalization of a Smale horseshoe in higher space dimensions is given by

DEFINITION 3 [15] Let $\Delta \subset U \subset \mathbf{R}^3$ be a rectangle and $f : U \rightarrow \mathbf{R}^3$ be a diffeomorphism. $\Delta \cap f(\Delta)$ is called a horseshoe if it contains at least two full components Δ_1 and Δ_2 such that for $\Delta' = \Delta_1 \cup \Delta_2$ the following conditions hold:

1. $\pi_2(\Delta') \subset \text{int}(D_2)$ and $\pi_1(f^{-1}(\Delta')) \subset \text{int}(D_1)$,
2. $D(f|_{f^{-1}(\Delta')})$ preserves and expands a horizontal cone family on $f^{-1}(\Delta')$,
3. $D(f|_{\Delta'}^{-1})$ preserves and expands a vertical cone family on Δ' .

To compute the return map P we will first prove that we can completely linearize the local maps.

LEMMA 4 *Suppose that the distinct eigenvalues of the linearisation A at 0 $\lambda_{1,2} = \frac{\mu_2}{2} \pm \sqrt{\frac{\mu_2^2}{4} + \mu_1}$ are not in resonance, i.e. $\lambda_i - (k\lambda_1 + l\lambda_2) \neq 0$ for $k, l \in \mathbf{N}, k + l > 1$. Then there exists a D_3 -equivariant smooth diffeomorphism H conjugating the flow Φ_t of (3) and $\exp(At)$ on some neighborhood U of the origin: $H\Phi_t = \exp(At)H$.*

Proof: We consider first the time-one-map Φ_1 , again the linear part is diagonal with eigenvalues $e^{\lambda_1}, e^{\lambda_2}$. For these the non-resonance conditions for maps $\exp \lambda_i \neq \exp(k\lambda_1) \cdot \exp(l\lambda_2)$ for $k, l \in \mathbf{N}, k + l > 1$ hold. The non-resonance conditions imply that we can formally remove all terms of algebraic order by a near-identity coordinate change. This is possible even in a D_3 -equivariant setting [11]. So we still have to remove flat terms and discuss convergence. To remove these flat terms we use a version of Sternberg's theorem [15, theorem 6.6.7]. The assumptions are fulfilled: The linear part is diagonal and the normal form which can be achieved by the above coordinate change is a convergent power series, since it is only linear. The theorem then gives the existence of a smooth diffeomorphism conjugating Φ_1 and its normal form. Thus there exists a smooth diffeomorphism H_1 linearizing Φ_1 in a neighborhood of the origin. Furthermore the construction in [15] can be chosen to preserve D_3 -equivariance, when we use invariant cut-off functions. Then the D_3 -equivariant diffeomorphism $H = \int_0^1 \exp(-At)H_1\Phi_t dt$ is the needed conjugacy for the entire flow on some neighborhood U of 0. This can be seen when using $\exp(-A)H_1\Phi_1 = H_1$

$$\begin{aligned} \exp(-As)H\Phi_s &= \int_0^1 \exp(-A(t+s))H_1\Phi_{t+s} dt = \int_s^{s+1} \exp(-Au)H_1\Phi_u du \\ &= H - \int_0^s \exp(-Au)H_1\Phi_u du + \int_1^{s+1} \exp(-Au)H_1\Phi_u du \\ &= H - \int_0^s \exp(-A(u+1))H_1\Phi_{u+1} du + \int_1^{s+1} \exp(-Au)H_1\Phi_u du \\ &= H \square \end{aligned}$$

Now we can compute the map P . After the coordinate change of the lemma the local maps are given by a linear flow. Then the stable and unstable manifolds coincide with the stable and unstable eigenspaces. To carry out the analysis we use again the scaled coordinates $x = x_1 + ix_2, y = y_1 + iy_2 \in \mathbf{C}$ for some $\epsilon > 0$ small. We know the homoclinic orbits explicitly by section 3 up to perturbations of order $O(\epsilon)$. While neglecting terms of order $O(\epsilon^2)$ the system in \mathbf{C}^2 is given by equation (6).

LOCAL MAPS: To compute the local maps we use a basis of eigenvectors of the linearized system: For the eigenvalue $\lambda_1 = \frac{\epsilon\nu_2}{2} + \sqrt{\frac{\epsilon^2\nu_2^2}{4} + \nu_1} > 0$ we choose v_1, v_2 and for the eigenvalue $\lambda_2 = \frac{\epsilon\nu_2}{2} - \sqrt{\frac{\epsilon^2\nu_2^2}{4} + \nu_1} < 0$ the vectors v_3, v_4 . The original basis of $\mathbf{R}^4 \cong \mathbf{C}^2$ is given by (x_1, y_1, x_2, y_2) .

$$\begin{aligned} v_1 &= (1 + \lambda_1^2)^{-\frac{1}{2}}(1, \lambda_1, 0, 0)^T, & v_2 &= (1 + \lambda_1^2)^{-\frac{1}{2}}(0, 0, 1, \lambda_1)^T, \\ v_3 &= (1 + \lambda_2^2)^{-\frac{1}{2}}(1, \lambda_2, 0, 0)^T, & v_4 &= (1 + \lambda_2^2)^{-\frac{1}{2}}(0, 0, 1, \lambda_2)^T. \end{aligned}$$

A vector $a \in \mathbf{R}^4$ is then denoted as $a = a_1v_1 + a_2v_2 + a_3v_3 + a_4v_4$. The

eigenvectors v_1 and v_3 span $\text{Fix}(\kappa)$. The section S_1^{out} is then defined by

$$a_1 = -c \text{ and } \max\{|a_2|, |a_3|, |a_4|\} < \delta$$

with c small and $0 < \delta \ll c$ such that the section is completely inside U , where the flow is linearized. S_1^{in} is given by

$$a_3 = -c \text{ and } \max\{|a_1|, |a_2|, |a_4|\} < \delta.$$

We will also use rotated coordinate systems with basis vectors $v'_l = \gamma v_l$ and $v''_l = \gamma^2 v_l$ with coefficients a'_l, a''_l . Thus we can define the sections of the rotated homoclinic orbits.

$$\begin{aligned} S_2^{out} &: a'_1 = -c, \max\{|a'_2|, |a'_3|, |a'_4|\} < \delta \\ S_3^{out} &: a''_1 = -c, \max\{|a''_2|, |a''_3|, |a''_4|\} < \delta \\ S_2^{in} &: a'_3 = -c, \max\{|a'_1|, |a'_2|, |a'_4|\} < \delta \\ S_3^{in} &: a''_3 = -c, \max\{|a''_1|, |a''_2|, |a''_4|\} < \delta \end{aligned}$$

First we compute $P_l^{loc}, l \in \{1, 2, 3\}$. The flow of the linear system is given by

$$\Phi_t(a) = a_1 v_1 e^{\lambda_1 t} + a_2 v_2 e^{\lambda_1 t} + a_3 v_3 e^{\lambda_2 t} + a_4 v_4 e^{\lambda_2 t}, \quad (7)$$

similarly in the primed versions for the rotated coordinate systems. Starting at a vector $a \in S_1^{in} \cup S_2^{in} \cup S_3^{in}$ with $P_l^{loc}(a) \in S_1^{out}$ (i.e. especially $a_1 < 0$), the time $t = (\ln \frac{c}{|a_1|})/\lambda_1$ is needed to reach the S_1^{out} section. Then $P_l^{loc}(a_1 v_1 + a_2 v_2 + a_3 v_3 + a_4 v_4)$

$$= (-c v_1 + a_2 \left| \frac{c}{a_1} \right| v_2 + a_3 \left| \frac{a_1}{c} \right|^{\frac{|\lambda_2|}{\lambda_1}} v_3 + a_4 \left| \frac{a_1}{c} \right|^{\frac{|\lambda_2|}{\lambda_1}} v_4) \quad (8)$$

with $\frac{|\lambda_2|}{\lambda_1} = 1 + \frac{18}{49} \epsilon^2 \nu_1 + \frac{6}{7} \epsilon \sqrt{\frac{9}{49} \epsilon^2 \nu_1^2 + \nu_1} + O(\epsilon^3)$.

To understand the geometry of the local maps we compute how the preimage of the 'out'-sections $S_l^{out}, l \in \{1, 2, 3\}$ intersects the 'in'-sections $S_l^{in}, l \in \{1, 2, 3\}$ and how the images of S_l^{in} intersect the 'out'-sections S_l^{out} . We start with the preimage of S_1^{out} intersected with S_1^{in}

$$\begin{aligned} & S_{1,1}^{in} \\ &= S_1^{in} \cap P_1^{loc^{-1}}(S_1^{out}) \\ &= \{(a_1, a_2, a_3, a_4) | a_3 = -c, \max\{|a_1|, |a_2|, |a_4|\} < \delta\} \\ &\cap \{(a_1, a_2, a_3, a_4) | a_1 < 0, \max\{|a_2| \left| \frac{c}{a_1} \right|, |a_3| \left| \frac{a_1}{c} \right|^{\frac{|\lambda_2|}{\lambda_1}}, |a_4| \left| \frac{a_1}{c} \right|^{\frac{|\lambda_2|}{\lambda_1}}\} < \delta\} \\ &= \{(a_1, a_2, a_3, a_4) | -\delta < a_1 < 0, |a_2| < \delta \left| \frac{a_1}{c} \right|, a_3 = -c, |a_4| < \delta\}. \end{aligned}$$

This is the slab with label '1' in figure 5. Then the image of S_1^{in} inside S_1^{out} is given by $S_1^{out} \cap P_1^{loc}(S_1^{in}) = P_1^{loc}(S_{1,1}^{in})$

$$= \{(a_1, a_2, a_3, a_4) | a_1 = -c, |a_2| < \delta, -\delta \frac{|\lambda_2|}{\lambda_1} < a_3 < 0, |a_4| < \frac{\delta}{c} |a_3|\}.$$

This set is the slab with label ‘1’ in figure 4. To determine the images $P_2^{loc}(S_2^{in}) \cap S_1^{out}$ and $P_3^{loc}(S_3^{in}) \cap S_1^{out}$ we have just to rotate a part of the coordinate system. Inside the stable eigenspace (v_3, v_4) is changed to (v'_3, v'_4) and (v''_3, v''_4) respectively. Equation (7) holds for each eigenspace independently. Thus the restrictions are essentially the same as for $S_1^{out} \cap P_1^{loc}(S_1^{in})$ just with a'_3, a'_4 and a''_3, a''_4 instead of a_3, a_4 . Hence the slab $S_1^{out} \cap P_1^{loc}(S_1^{in})$ has just to be rotated by $2\pi/3$ and $4\pi/3$ inside the (v_3, v_4) plane to get $S_1^{out} \cap P_2^{loc}(S_2^{in})$ and $S_1^{out} \cap P_3^{loc}(S_3^{in})$. A sketch of section S_1^{out} with the images of $S_l^{in}, l \in \{1, 2, 3\}$ is given in figure 4.

Next we will compute the preimage of S_2^{out} and S_3^{out} under P_1^{loc} to get the structure of S_1^{in} . When we use a rotated coordinate system (v'_1, v'_2) instead of (v_1, v_2) inside the unstable eigenspace, the time $t = (\ln \frac{c}{|a'_1|})/\lambda_1$ is needed to reach S_2^{out} . This yields to

$$\begin{aligned} & P_1^{loc}(a'_1 v'_1 + a'_2 v'_2 - cv_3 + a_4 v_4) \\ = & (-cv'_1 + a'_2 \left| \frac{c}{a'_1} \right| v'_2 - c \left| \frac{a'_1}{c} \right|^{\frac{|\lambda_2|}{\lambda_1}} v_3 + a_4 \left| \frac{a'_1}{c} \right|^{\frac{|\lambda_2|}{\lambda_1}} v_4). \end{aligned}$$

So the preimage of S_2^{out} under P_1^{loc} is just $S_{1,1}^{in}$ rotated by $2\pi/3$ inside the unstable eigenspace. And finally for the preimage of S_3^{out} the coordinate system has to be rotated by $4\pi/3$ in the unstable eigenspace. The section S_1^{in} with the preimages of $S_l^{out}, l \in \{1, 2, 3\}$ is drawn in figure 5.

GLOBAL MAPS: Next we approximate $P_l^{glo} : S_l^{out} \rightarrow S_l^{in}$ by an Taylor expansion using the linearisation along the homoclinic orbit. This approximation is valid by a general perturbation argument for hyperbolic sets, when we choose the size of the cubes δ small enough. We get a constant term of the global map when considering the splitting of the homoclinic orbit. The point $(-c, 0, 0, 0) \in S_1^{out}$ is inside $\text{Fix}(\kappa)$, hence it will be mapped to $S_1^{in} \cap \text{Fix}(\kappa)$. Thus the constant term is the distance of the stable and unstable manifolds inside $\text{Fix}(\kappa)$. Using [13, Eq.(4.5.11)] this distance is given by $d(\nu_2, \epsilon) = \frac{\epsilon M(\nu_2)}{\|f(q)\|} + O(\epsilon^2)$, with Melnikov functional $M(\nu_2)$ and vector field f on $\text{Fix}(\kappa)$. For our system this is $d(\nu_2) = \epsilon \frac{4}{5c} \sqrt{\nu_1}(\nu_2 + \frac{6}{7}\nu_1)$.

In (x_1, y_1, x_2, y_2) coordinates the linearisation along the homoclinic solution for $\epsilon > 0$ is given by $B = D_{(x,y)} f|_{(x(t), y(t))} =$

$$\begin{pmatrix} 0 & 1 & 0 & 0 \\ \nu_1 + 2x_1(t) - \epsilon y_1(t) & \epsilon(\nu_2 - x_1(t)) & 0 & 0 \\ 0 & 0 & 0 & 1 \\ 0 & 0 & \nu_1 - 2x_1(t) + \epsilon y_1(t) & \epsilon(\nu_2 + x_1(t)) \end{pmatrix}, \tag{9}$$

where $x_1(t), y_1(t)$ are the non-zero components of the homoclinic orbit. This means that we have to solve the non-autonomous linear differential equation $\dot{\xi} = B\xi$. We use the block diagonal structure of the matrix. The first block describes the behavior inside the invariant subspace $\text{Fix}(\kappa)$ and the second block the orthogonal complement $\text{Fix}(\kappa)^\perp$.

In the first block we are interested in the initial values $\xi_0 = a_3 v_3$ inside S_1^{out} . One solution of the variational equation inside $\text{Fix}(\kappa)$ is given by $\dot{q}_0(t)$ for $\epsilon = 0$. Letting $q_0(0) \in S_1^{out}$ and $q_0(T) \in S_1^{in}$, then $\|q_0(0)\| = \|q_0(T)\|$ by symmetry. The vectors $\xi_0, \dot{q}_0(0)$ restricted to $\text{Fix}(\kappa)$ are a fundamental system. The Wronskian W of this system is constant by Liouville's theorem: $\dot{W} = \text{trace}(B|_{\text{Fix}(\kappa)})W = 0$. Therefore, as $\dot{q}_0(0) = kv_1$ and $\dot{q}_0(T) = kv_3$, the projection of $\xi_0(T)$ onto v_1 is a_3 . By smooth dependence on parameters this yields to $P_1^{glo}(a_3 v_3) = (1 + O(\epsilon))a_3 v_1$.

In the second block we consider initial values $\xi_1 = a_2 v_2$ and $\xi_2 = a_4 v_4$. First assume that $\epsilon = 0$. As $(\nu_1 - 2x_1(t)) > \nu_1 > 0$ and $\xi_1^{(1)}(0), \xi_1^{(2)}(0) > 0$ hold, the two components $\xi_1^{(1)}(t)$ and $\xi_1^{(2)}(t)$ are increasing. The global map also expands this vector for $\epsilon > 0$ by the smooth dependence on the parameter ϵ for finite time. Hence in linear approximation we get $P_1^{glo}(a_2 v_2) = a_2(\alpha_1 v_2 + \alpha_2 v_4)$ with $\alpha_1^2 + \alpha_2^2 \geq 1$. Furthermore

$$\alpha_1 \geq 0.9|\alpha_2| \tag{10}$$

holds because the coefficients of the solution are positive in the x_2, y_2 coordinates. Applying Liouville's theorem again for $\epsilon = 0$, the second initial vector is mapped to $P_1^{glo}(a_4 v_4) = a_4(\beta_1 v_2 + \beta_2 v_4)$ with $\alpha_1 \beta_2 - \alpha_2 \beta_1 = 1$. Again $\epsilon > 0$ will give perturbations of type $1 + O(\epsilon)$, which we will suppress by still using the same notation.

FULL MAP: We now consider only those points which are mapped under the local maps from $S_1^{in} \cup S_2^{in} \cup S_3^{in}$ to S_1^{out} . When we use (v_1, v_2, v_3, v_4) as a coordinate system for all three 'in'-sections then the composed mapping is given by

$$P_1^{glo} \circ P_l^{loc} : S_l^{in} \rightarrow S_1^{in}, l \in \{1, 2, 3\}$$

$$\begin{pmatrix} a_1 \\ a_2 \\ a_3 \\ a_4 \end{pmatrix} \mapsto \begin{pmatrix} \frac{4\epsilon}{5c} \sqrt{\nu_1} (\frac{6}{7}\nu_1 + \nu_2) + (1 + O(\epsilon))a_3 \left| \frac{a_1}{c} \right|^{1+\frac{6}{7}\epsilon\sqrt{\nu_1}} \\ \alpha_1 a_2 \left| \frac{c}{a_1} \right| + \beta_1 a_4 \left| \frac{a_1}{c} \right|^{1+\frac{6}{7}\epsilon\sqrt{\nu_1}} \\ -c \\ \alpha_2 a_2 \left| \frac{c}{a_1} \right| + \beta_2 a_4 \left| \frac{a_1}{c} \right|^{1+\frac{6}{7}\epsilon\sqrt{\nu_1}} \end{pmatrix} \tag{11}$$

Now we can use this to determine the return map $P : S_1^{in} \cup S_2^{in} \cup S_3^{in} \rightarrow S_1^{in} \cup S_2^{in} \cup S_3^{in}$, where it is defined. Because of the symmetry the maps $P_2^{glo} \circ P_l^{loc}$ and $P_3^{glo} \circ P_l^{loc}$ are related to (11) by simple rotations of whole \mathbf{R}^4 . When changing to the rotated coordinates, the maps $P_2^{glo} \circ P_l^{loc}$ and $P_3^{glo} \circ P_l^{loc}$ are given by equation (11) with a_i replaced by a'_i and a''_i . Therefore it is enough to consider a reduced map \tilde{P} just as a map from one section S^{in} to itself. We just have to change the original labels '1', '2' and '3' in the S_2^{in} and S_3^{in} sections. We will use a labeling relative to our position and call our position '1', the next homoclinic orbit in the direction of the rotation is called '2' and the other one '3'.

PROOF OF THEOREM 1: The existence of a horseshoe for this reduced map \tilde{P} will be shown. Analyzing the implications for the full map will prove the

theorem. The conditions of definition 3 will be checked for the map:

$$\tilde{P} : S^{in} \rightarrow S^{in}$$

$$\begin{pmatrix} a_1 \\ a_2 \\ a_4 \end{pmatrix} \mapsto \begin{pmatrix} \frac{4\epsilon}{5c} \sqrt{\nu_1} (\frac{6}{7}\nu_1 + \nu_2) + (1 + O(\epsilon)) |a_1| \left| \frac{a_1}{c} \right|^{\frac{6}{7}\epsilon \sqrt{\nu_1}} \\ \alpha_1 a_2 \left| \frac{c}{a_1} \right| + \beta_1 a_4 \left| \frac{a_1}{c} \right|^{1 + \frac{6}{7}\epsilon \sqrt{\nu_1}} \\ \alpha_2 a_2 \left| \frac{c}{a_1} \right| + \beta_2 a_4 \left| \frac{a_1}{c} \right|^{1 + \frac{6}{7}\epsilon \sqrt{\nu_1}} \end{pmatrix}. \quad (12)$$

The horizontal direction is $\alpha_1 v_2 + \alpha_2 v_4$ and the vertical directions are v_1 and v_4 . Using these as a new basis with coefficients ζ_1, ζ_2 and ζ_3 we define Δ as the product of discs with radii 2δ in ζ_1 for D_1 and δ in (ζ_2, ζ_3) for D_2 with the further restriction $\frac{\delta}{6} < \zeta_2 < \frac{\delta}{3}$. This means we choose a coordinate system such that we can ignore any rotation of figure 4 under the global mapping to figure 5, even if $|\alpha_2|$ is not small. This can be done, because we estimated $\alpha_1 \geq 0.9|\alpha_2|$ in (10). We just have to change the labels from a_2 to ζ_1 , a_1 to ζ_2 and a_4 to ζ_3 . As above we denote the rotated coordinates by ζ'_i and ζ''_i . The rectangle is given in figure 6. We choose the distance of splitting $d = \frac{\delta}{6}$. The two full components Δ_1 and Δ_2 , which have to be contained in $\Delta \cap \tilde{P}(\Delta)$, are the two top dotted slabs in figure 6.

We consider the preimages of these two slabs under the original return map P , i.e. we are interested in the preimages of $\Delta_1, \Delta_2 \subset S_1^{in}$ under $P_1^{glo} \circ P_{2,3}^{loc}$. Then we get $(P_1^{glo} \circ P_2^{loc})^{-1}(\Delta_1) =$

$$\tilde{\Gamma}_1 = \{(\zeta_1, \zeta_2, \zeta'_3) \in \gamma \cdot \Delta \mid 0 < -\zeta_2 < 2\delta, |\zeta_1| \leq \delta \left| \frac{\zeta_2}{c\alpha_1} \right|\} \subset \gamma\Delta \subset S_2^{in}$$

and similarly $(P_1^{glo} \circ P_3^{loc})^{-1}(\Delta_2) =$

$$\tilde{\Gamma}_2 = \{(\zeta_1, \zeta_2, \zeta''_3) \in \gamma^2 \cdot \Delta \mid 0 < -\zeta_2 < 2\delta, |\zeta_1| \leq \delta \left| \frac{\zeta_2}{c\alpha_1} \right|\} \subset \gamma^2\Delta \subset S_3^{in}.$$

As we identified the three sections in this analysis of \tilde{P} , we deal with Γ_1 and Γ_2 , which are contained in the slabs with labels 2 and 3 in figure 6. The further restrictions are due to the possible additional expanding of the global map, i.e. the slabs are defined by

$$\Gamma_1 = \gamma^{-1}\tilde{\Gamma}_1 = \{(\zeta''_1, \zeta''_2, \zeta_3) \in \Delta \mid 0 < -\zeta''_2 < 2\delta, |\zeta''_1| \leq \delta \left| \frac{\zeta''_2}{c\alpha_1} \right|\}. \quad (13)$$

$$\Gamma_2 = \gamma^{-2}\tilde{\Gamma}_2 = \{(\zeta'_1, \zeta'_2, \zeta_3) \in \Delta \mid 0 < -\zeta'_2 < 2\delta, |\zeta'_1| \leq \delta \left| \frac{\zeta'_2}{c\alpha_1} \right|\}, \quad (14)$$

After relabeling we have $\Delta_1 = \tilde{P}(\Gamma_1)$ and $\Delta_2 = \tilde{P}(\Gamma_2)$: The slab Γ_1 is mapped by P_1^{loc} to S_3^{out} and then by P_3^{glo} , because of our relabeling it will be the slab coming from S_2^{out} , hence it is the dotted slab with label 2 and therefore $\Delta_1 = \tilde{P}(\Gamma_1)$. In the same manner we get $\Delta_2 = \tilde{P}(\Gamma_2)$.

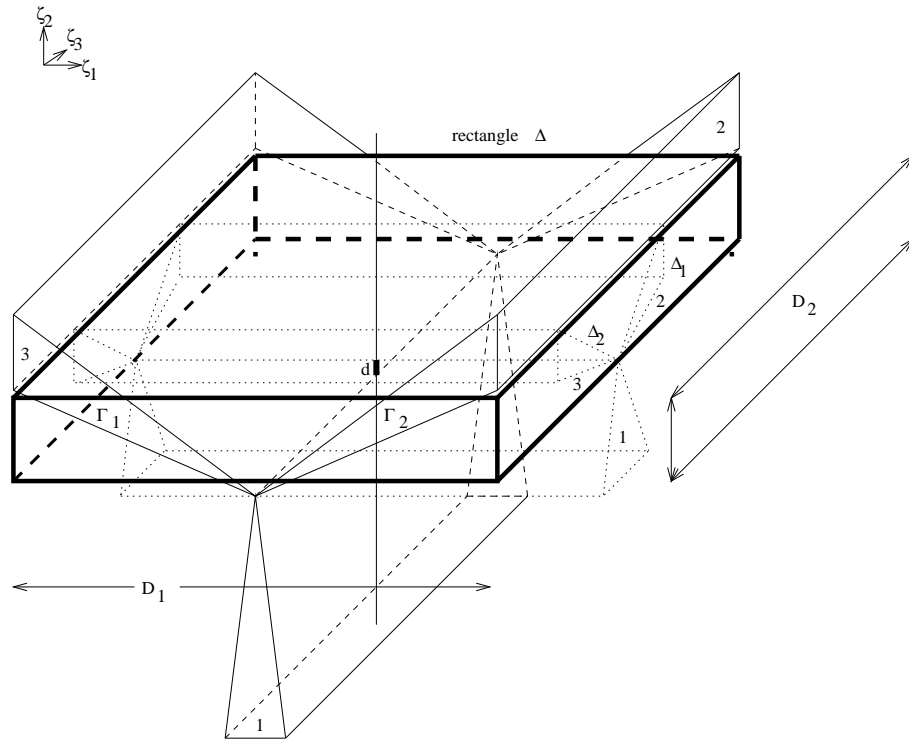


Figure 6: The section S^{in} with rectangle $\Delta = D_1 \times D_2$ including $\Delta_{1,2} = \tilde{P}(\Gamma_{1,2})$

So we can now check the conditions in the definition of the horseshoe. The two components $\Delta_1 = P(\Gamma_1)$ and $\Delta_2 = P(\Gamma_2)$ are full: $\pi_2(\Gamma_i) = D_2$ for $i = 1, 2$, because we can choose ζ_3 freely and $\zeta_2' < 0$ (respective ζ_2'') freely with $|\zeta_1'|$ (respective ζ_1'') small inside Δ , i.e. we get all wanted $\zeta_2 > 0$ in the definition of Γ_i . For all $\zeta \in \Gamma_i$ the restriction $\pi_1|_{f(\Gamma_i \cap (D_1 \times \pi_2(\zeta)))}$ is a bijection onto D_1 . When we vary ζ_1 for any given $z = (a_1, \alpha_1 \zeta_1, \alpha_2 \zeta_1 + a_4) \in \Gamma_i$ then P is affine linear (see (12)) and the projection π_1 to the ζ_1 component is injective, which is the a_2 component in P . It is also surjective onto D_1 , because the restrictions on a_2 inside Γ_i ((14) and (13)) were given such that the maximal modulus of the a_2 component is δ in the image.

Next we check the first condition in definition 3. $\pi_2(\Delta') \subset \text{int}(D_2)$ holds because of the contraction in the $a_1 = \zeta_2$ and ζ_3 component when choosing $\frac{6}{7}\nu_1 + \nu_2$ small enough. The ζ_3 component is given by

$$\left| (\alpha_1 \zeta_3 - \alpha_2 \zeta_1) \left| \frac{\zeta_2}{c} \right|^{1 + \frac{6}{7}\epsilon \sqrt{\nu_1}} \right| \ll \delta.$$

The other condition $\pi_1(P^{-1}\Delta') \subset \text{int}(D_1)$ also holds, because $|\zeta_1| \leq |\zeta_1''|/2 +$

$\sqrt{3}|\zeta_2''|/2$ and ζ_1', ζ_2' and ζ_1'', ζ_2'' are small enough by the definition of Γ_1 and Γ_2 (see (14),(13)).

Finally we have to check the cone conditions, for which we need the linearizations of \tilde{P} and \tilde{P}^{-1} . Suppressing all factors $1 + O(\epsilon)$ these are given in the original (a_1, a_2, a_4) coordinates by $D\tilde{P}_x(a_1, a_2, a_4) =$

$$\begin{pmatrix} -\left|\frac{a_1}{c}\right|^{\frac{6}{7}\epsilon\sqrt{\nu_1}} & 0 & 0 \\ \alpha_1 a_2 \frac{c}{a_1^2} - \beta_1 a_4 \left|\frac{a_1}{c}\right|^{\frac{6}{7}\epsilon\sqrt{\nu_1}} & \alpha_1 \left|\frac{c}{a_1}\right| & \beta \left|\frac{a_1}{c}\right|^{1+\frac{6}{7}\epsilon\sqrt{\nu_1}} \\ \alpha_2 a_2 \frac{c}{a_1^2} - \beta_2 a_4 \left|\frac{a_1}{c}\right|^{\frac{6}{7}\epsilon\sqrt{\nu_1}} & \alpha_2 \left|\frac{c}{a_1}\right| & \beta_2 \left|\frac{a_1}{c}\right|^{1+\frac{6}{7}\epsilon\sqrt{\nu_1}} \end{pmatrix} \quad (15)$$

and if $(a_1, a_2, a_4) = \tilde{P}^{-1}(z)$ then $D\tilde{P}_x^{-1}(z) = (D\tilde{P}_x(a_1, a_2, a_4))^{-1}$ is

$$\begin{pmatrix} -\left|\frac{c}{a_1}\right|^{\frac{6}{7}\epsilon\sqrt{\nu_1}} & 0 & 0 \\ -\frac{a_2}{a_1} \left|\frac{c}{a_1}\right|^{1-\frac{6}{7}\epsilon\sqrt{\nu_1}} a_2 & \beta_2 \left|\frac{a_1}{c}\right| & -\beta \left|\frac{a_1}{c}\right| \\ -a_4 \left|\frac{c}{a_1}\right|^{1+\frac{6}{7}\epsilon\sqrt{\nu_1}} & -\alpha_2 \left|\frac{c}{a_1}\right|^{1+\frac{6}{7}\epsilon\sqrt{\nu_1}} & \alpha \left|\frac{c}{a_1}\right|^{1+\frac{6}{7}\epsilon\sqrt{\nu_1}} \end{pmatrix}. \quad (16)$$

Changing to the new ζ coordinates, we can easily check the cone conditions: The matrix $D\tilde{P}(\zeta_2, \zeta_1, \zeta_3)$ is given by

$$\begin{pmatrix} -\left|\frac{\zeta_2}{c}\right|^{\frac{6}{7}\epsilon\sqrt{\nu_1}} & 0 & 0 \\ \frac{\zeta_1}{\alpha_1} \frac{c}{\zeta_2} - (\alpha_1 \zeta_3 - \alpha_2 \zeta_1) \frac{\beta_1}{\alpha_1} \left|\frac{\zeta_2}{c}\right|^{\frac{6}{7}\epsilon\sqrt{\nu_1}} & \alpha_1 \left|\frac{c}{\zeta_2} + \frac{\alpha_2}{\alpha_1} \left|\frac{\zeta_2}{c}\right|^{1+\frac{6}{7}\epsilon\sqrt{\nu_1}}\right. & \left. \frac{\beta_1}{\alpha_1} \left|\frac{\zeta_2}{c}\right|^{1+\frac{6}{7}\epsilon\sqrt{\nu_1}}\right. \\ -(\alpha_1 \zeta_3 - \alpha_2 \zeta_1) \left|\frac{\zeta_2}{c}\right|^{\frac{6}{7}\epsilon\sqrt{\nu_1}} & \left. \alpha_2 \left|\frac{\zeta_2}{c}\right|^{1+\frac{6}{7}\epsilon\sqrt{\nu_1}}\right. & \left. \left|\frac{\zeta_2}{c}\right|^{1+\frac{6}{7}\epsilon\sqrt{\nu_1}}\right. \end{pmatrix} \quad (17)$$

and $D\tilde{P}^{-1}$ by

$$\begin{pmatrix} -\left|\frac{c}{\zeta_2}\right|^{\frac{6}{7}\epsilon\sqrt{\nu_1}} & 0 & 0 \\ -\left|\frac{c}{\zeta_2}\right|^{\frac{6}{7}\epsilon\sqrt{\nu_1}} \frac{\zeta_1}{\zeta_2 \alpha_1^2} & \left|\frac{\zeta_2}{c \alpha_1}\right| & -\frac{\beta_1}{\alpha_1} \left|\frac{\zeta_2}{c}\right| \\ \left(\frac{\alpha_2 \zeta_1}{c} - \alpha_1 (\alpha_1 \zeta_3 - \alpha_2 \zeta_1)\right) \left|\frac{c}{\zeta_2}\right|^{1+\frac{6}{7}\epsilon\sqrt{\nu_1}} & -\alpha_2 \left|\frac{c}{\zeta_2}\right|^{1+\frac{6}{7}\epsilon\sqrt{\nu_1}} & \alpha_1^2 \left|\frac{c}{\zeta_2}\right|^{1+\frac{6}{7}\epsilon\sqrt{\nu_1}} + \beta_1 \alpha_2 \left|\frac{\zeta_2}{c}\right| \end{pmatrix}. \quad (18)$$

Now it is straightforward to see, that the term $\alpha_1 \left|\frac{c}{\zeta_2}\right|$ is the largest entry in the matrix (17). Then it preserves horizontal cones with constant e.g. $s = 0.3$ and expands them with expansion rate $\mu = \alpha_1 \frac{c}{2\delta} > 1$. Similar we see, that $\alpha_1^2 \left|\frac{c}{\zeta_2}\right|^{1+\frac{6}{7}\epsilon\sqrt{\nu_1}}$ is the leading term of the last two lines in (18). Hence it preserves vertical cones with constants $s = 0.3$ and expands them with constant λ^{-1} for $\lambda = 2 \frac{\delta}{c} \frac{6}{7} \epsilon \sqrt{\nu_1} < 1$.

By Katok and Hasselblatt [15, p.274] we have the existence of an invariant hyperbolic Cantor set for the reduced map \tilde{P} , such that the dynamics are

topological conjugate to the shift on two symbols for this reduced map. Then for the complete return map P there exists the shift of finite type with the transition matrix of the theorem: if an orbit is near the loop l in the present, then as the shift is on the symbols 2 and 3 the next loop in the itinerary has to be $l + 1 \bmod 3$ or $l + 2 \bmod 3$. Similarly the previous one was $l + 1 \bmod 3$ or $l + 2 \bmod 3$. Thus possible sequences $(x_n)_{n \in \mathbf{Z}}$ have the form $x_n \neq x_{n+1}$. The realization of all these sequences are guaranteed by the existence of the full shift on two symbols for \tilde{P} . Proposition 6.5.3 in [15] gives then even persistence under small C^1 perturbations i.e. for an open set in parameter space. Hence we can include higher order terms. This also verifies the linear approximation of the global maps, for which all equivariant higher order terms can be neglected. It remains to check the symmetry properties of C , P and τ . The sections S_k^{in} are related by symmetry: $S_2^{in} = \gamma S_1^{in}$ and $S_3^{in} = \gamma^2 S_1^{in}$. Furthermore S_1^{in} is κ -invariant and $S_3^{in} = \kappa S_2^{in}$. Then P^{loc} is equivariant, because the linearizing diffeomorphism is D_3 -equivariant. The global part is equivariant under rotation γ by construction. It is equivariant under κ by the following argument:

$$\begin{aligned} \kappa^{-1} P^{gl_o} \kappa x &= \kappa^{-1} \Phi_{t(\kappa x)}(\kappa x) = \Phi_{t(\kappa x)}(x) \\ P^{gl_o} x &= \Phi_{t(x)}(x) \end{aligned}$$

As the times $t(\kappa x)$ and $t(x)$ are both close to the time needed of the homoclinic orbits from the ‘out’ section to the ‘in’ section, we get $t(\kappa x) \approx t(x)$. As $\Phi_{t(x)}(x), \Phi_{t(\kappa x)}(x) \in S_k^{in}$ for the same k , we get $t(x) = t(\kappa x)$. Hence P^{gl_o} and P are equivariant. Then $C = \bigcap_{n=-\infty}^{\infty} P^n(\bigcup_{i=1,2,3} S_i^{in})$ is D_3 invariant, because P^n is equivariant and $\bigcup_{i=1,2,3} S_i^{in}$ is invariant. If $x \in C$ and $x = P^n(a_n)$ with $a_n \in S_{x_n}^{in}$, then $\tau(x) = (x_n)_{n \in \mathbf{Z}}$ and the equivariance of τ can be easily checked using the representations (2) and (1). \square

5 DISCUSSION

In this section we give a more complete bifurcation diagram of the Takens-Bogdanov point with D_3 -symmetry, using numerical studies of the normal form equations. Then we will describe an application to coupled oscillators.

A major drawback in all further numerical studies is that there are not any stable dynamic features except the origin for some parameter values ($\mu_1, \mu_2 < 0$). Therefore all direct simulations will not give much insight. Some conjectures about the periodic solutions created at Hopf bifurcations are possible using the path-following program AUTO [5].

The dynamics are fully understood in the invariant plane $\text{Fix}(\kappa)$ by [14], see also [16]. There are two branches of periodic orbits starting from the D_3 -Hopf bifurcation of 0 and the Hopf of N_1 at $\mu_2 = -\mu_1, \mu_1 > 0$. These branches do not undergo any folds and end at the homoclinic orbit. The global behavior of the other branches of periodic solutions are analyzed using AUTO. These branches of periodic solutions outside $\text{Fix}(\kappa)$ seem to break down at the clover

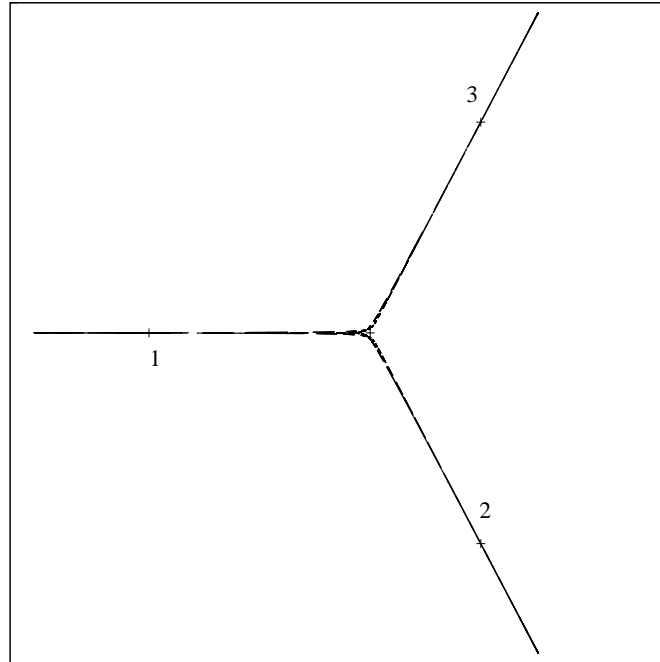


Figure 7: A periodic orbit with sequence 1213 of isotropy type $\tilde{\mathbf{Z}}_2$ of the branch coming from the D_3 -Hopf. Parameter values are near the existence of the homoclinic clover. A projection on the v plane is shown, the crosses denote steady states. The trajectory of periodic orbit was approximated by integrating the differential equation starting at points, which described the periodic solution for AUTO.

structure of homoclinic orbits. Probably they are some of the periodic orbits of the subshift:

- The periodic solutions with isotropy type $\tilde{\mathbf{Z}}_2$ coming from the D_3 -Hopf bifurcation have period 4 created by the sequences 1213, 2321 and 3132, see figure 7.
- The solutions coming from the Hopf bifurcation of $N_{1,2,3}$ at $\mu_2 = \mu_1, \mu_1 < 0$ seem to have period 2, see figure 8.
- Even if the author could not pick up the $\tilde{\mathbf{Z}}_3$ periodic solutions starting at the D_3 -Hopf bifurcation for path-following with AUTO. We might conjecture that this branch also ends at the homoclinic clover. They are probably of period 3 with sequences 123 and 132.

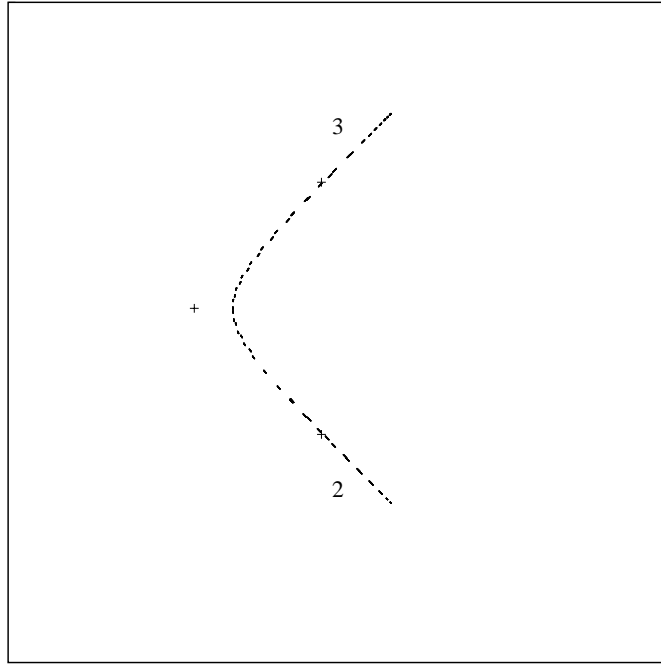


Figure 8: A periodic solution with sequence 23 with isotropy type $\tilde{\mathbf{Z}}_2$ on the branch coming from the Hopf bifurcation of N_1 .

The entire horseshoe does persist for some parameter by a general perturbation argument for hyperbolic sets. It remains an open question how long for example the other periodic orbits created by the horseshoe persist. This will probably involve even more complicated bifurcations.

We will consider an application to three coupled oscillators following Fiedler [6]. The system is given by

$$\dot{x}_i = f(x_i) + D(x_{i-1} + x_{i+1} - 2x_i) \pmod{3}, i = 1, 2, 3, \quad (19)$$

where $x_i \in \mathbf{R}^k$ and $D = \text{diag}(d_1, \dots, d_k)$. This system is equivariant under permutations of x_1, x_2 and x_3 . The symmetry group is isomorphic to D_3 . If we have a homogeneous solution, it will stay homogeneous under the evolution of time. We change to (x, y, z) coordinates where

$$x = x_1 + x_2 + x_3, y = x_1 - x_2, z = x_2 - x_3.$$

In the new coordinate system we then have:

$$\begin{aligned} \dot{x} &= f\left(\frac{x+z+2y}{3}\right) + f\left(\frac{x+z-y}{3}\right) + f\left(\frac{x-y-2z}{3}\right) \\ \dot{y} &= f\left(\frac{x+z+2y}{3}\right) - f\left(\frac{x+z-y}{3}\right) - 3Dy \\ \dot{z} &= f\left(\frac{x+z-y}{3}\right) - f\left(\frac{x-y-2z}{3}\right) - 3Dz \end{aligned} \quad (20)$$

We consider the homogeneous equilibrium (x_0, x_0, x_0) with linearisation $f'(x_0) = A$. In the new coordinates the equilibrium is $(3x_0, 0, 0)$. Its Jacobian in the entire system is given by the block diagonal matrix $\text{diag}(A, A - 3D, A - 3D)$.

We choose $k = 2$ and for f the dynamics of the Brusselator as an easy example. It gives some insight into the possible behavior of chemical oscillator. So $f = (f_1, f_2)$ is given by $f_1(\xi_1, \xi_2) = a - (b+1)\xi_1 + \xi_1^2\xi_2$, $f_2(\xi_1, \xi_2) = b\xi_1 - \xi_1^2\xi_2$ with $a, b > 0$, the equilibrium is $x_0 = (a, \frac{b}{a})$ and $A = \begin{pmatrix} b-1 & a^2 \\ -b & -a^2 \end{pmatrix}$. We choose

$D = \frac{1}{3} \begin{pmatrix} \lambda_1 & 0 \\ 0 & \lambda_2 \end{pmatrix}$. Then $A - 3D$ has a double eigenvalues 0 if

$$\begin{aligned} \det(A - 3D) &= \lambda_1\lambda_2 + \lambda_1a^2 - \lambda_2(b-1) + a^2 = 0 \\ \text{trace}(A - 3D) &= b-1-a^2-\lambda_1-\lambda_2 = 0 \end{aligned}$$

The solution is given by $(\lambda_1, \lambda_2) = (b-1-a\sqrt{b}, -a^2+a\sqrt{b})$, the diffusion constants λ_1, λ_2 are positive and therefore somehow realistic for $a < \frac{b-1}{\sqrt{b}}$. So this D_3 -equivariant system has a Takens-Bogdanov point since there is a double zero eigenvalue and $A - 3D \neq 0$. We apply our bifurcation analysis for Takens-Bogdanov points with D_3 -symmetry to this problem. It will be valid on a four-dimensional center manifold which is tangent to the subspace spanned by y and z .

As $\text{trace}(A) > \text{trace}(A - 3D) = 0$ holds for $\lambda_1 + \lambda_2 > 0$, the matrix A has at least one eigenvalue with positive real part. Hence all dynamical features will be unstable if we consider the entire system. We could stabilize the system when using negative diffusion rates. But still all branching solutions have unstable directions due to the Takens-Bogdanov point making them inaccessible for direct numerical simulation.

The origin will still correspond to the homogeneous solution even after the needed coordinate changes. Then an interpretation of a D_3 -Hopf bifurcation in a ring of three coupled oscillators is given in [11, XVII.4]. The three different types of periodic solutions give different waveforms, phase shifts and resonances for the three cells. We furthermore expect near the bifurcation point the existence of inhomogeneous steady state solutions with two cells being in the same state. The periodic solutions coming from the Hopf bifurcations of these fixed points oscillate around these inhomogeneous steady states. In the first type two cells are in phase and in the other type two cells have a phase shift of

π . The periodic solutions collapse at the homoclinic orbits, since by moving in parameter space parts of the periodic orbits reach a state very close to the homogeneous equilibrium. For these parameter values the system is already ‘chaotic’ because of the existence of shift dynamics. When the solution follows one of the loops of the ‘clover’ structure it has nearly a \mathbf{Z}_2 symmetry, i.e. two cells have nearly the same state. Hence within the shift dynamics we have arbitrary changes of two out of three cells being nearly in phase. The structure of our subshift forces the system to change to another pair of cells being in phase after some time. Because of the unstable directions of the hyperbolic structure this behavior is only observable as a transient motion to infinity or to some stable solutions far away from the Takens-Bogdanov point.

ACKNOWLEDGMENTS

I would like to thank Peter Ashwin, Bernold Fiedler, Mark Roberts, Arnd Scheel and Ian Stewart for discussions.

REFERENCES

- [1] Armbruster, D., Guckenheimer, J. and Kim, S. [1989]. Chaotic dynamics in systems with square symmetry, *Physics Letters A* 140 no 7/8, p 416-420.
- [2] Arnold, V.I. [1983]. *Geometrical methods in the theory of ordinary differential equations*. Grundlehren der mathematischen Wissenschaften 250, Springer-Verlag, New York.
- [3] Bogdanov, R.I. [1975]. Versal deformations of a singular point on the plane in the case of zero eigenvalues. *Functional Anal. Appl.* (2)9, p 144-145.
- [4] Dangelmayr, G. and Knobloch, E. [1987]. The Takens-Bogdanov bifurcation with $O(2)$ symmetry. *Phil. Trans. R. Soc. London A* 322, p 243-279.
- [5] Doedel, E.J., Wang, X.J. and Fairgrieve, T. [1994]. *AUTO94 Software for continuation and bifurcation problems in ordinary differential equations*. California Institute of Technology.
- [6] Fiedler, B. [1986]. Global Hopf bifurcation of two-parameter flows, *Arch. Rational Mech. Anal.* 94, p 59-81.
- [7] Fiedler, B. [1996]. Global path following of homoclinic orbits in two-parameter flows, Pitman Math. Research Notes, No 352, p 79-146.
- [8] Field, M.J. [1983]. Isotopy and stability of equivariant diffeomorphisms, *Proc. London Math. Soc.* 46, p 487-516.
- [9] Gatermann, K. and Guyard, F. [1999] Gröbner bases, invariant theory and equivariant dynamics, *Journal of Symbolic Calculation* 27, p 1-28; program: URL: <http://www.zib.de/gatermann/symmetry.html>.

- [10] Glendeninning,P.[1994] *Stability, instability and Chaos*. Cambridge University Press.
- [11] Golubitsky,M., Stewart,I. and Schaeffer,D.G. [1988]. *Singularities and groups in bifurcation theory, volume II*.Appl.Math.Sci. 69,Springer-Verlag, New York.
- [12] Golubitsky,M., Swift,J.W. and Knobloch,E. [1984]. Symmetries and pattern selection in Rayleigh-Bénard convection,*Physica D* 10,p 249-276.
- [13] Guckenheimer,J. and Holmes,P. [1983].*Nonlinear oscillation, dynamical systems, and bifurcations of vector fields*. Appl.Math.Sci.42,Springer-Verlag, New York.
- [14] Hirschberg,P. and Knobloch,E.[1991]. An unfolding of the Takens-Bogdanov singularity.*Quart. Appl. Math.* 49, p 281-287.
- [15] Katok,A. and Hasselblatt,B.[1995]. *Introduction to the modern theory of dynamical systems*. Encyclopedia of mathematics and its applications v.54, Cambridge University Press.
- [16] Lari-Lavassani,A., Langford,W.F., Huseyin,K. and Gatermann,K.[1999]. Steady-state mode interactions for D_3 and D_4 -symmetric systems. *Dynamics of Continuous, Discrete and Impulsive Systems* 6,p 169–209.
- [17] Takens,F.[1974]. Singularities of vector fields, *Inst. Hautes Études Sci. Publ. Math.* 43, p 47-100.

Karsten Matthies
Institut für Mathematik I
Freie Universität Berlin
Arnimallee 2-6
D - 14195 Berlin
Germany
matthies@math.fu-berlin.de

